Algorithms to reduce the computational cost of vector Preisach model in view of Finite Element analysis

Riccardo Scorretti, Francesco Riganti-Fulginei, Antonino Laudani, Simone Quandam

Version of Record: https://www.sciencedirect.com/science/article/pii/S0304885321010829
Manuscript_fd592c21f005be648962e8323cb9d477

Algorithms to reduce the computational cost of vector Preisach model in view of Finite Element analysis

Scorretti Riccardo,[1] Francesco Riganti-Fulginei[2], Antonino Laudani[2], and Simone Quandam[3]

[1] Univ Lyon, Université Claude Bernard Lyon 1, INSA Lyon, ECLyon, CNRS, Ampère, F-69100, Villeurbanne, France.
[2] Department of Engineering, Roma Tre University, Via V. Volterra 62, 00146 Rome, Italy.
[3] Department of Engineering, University of Perugia, Via G. Duranti 93, 06125 Perugia, Italy.

Correspondence should be addressed to Riccardo Scorretti; riccardo.scorretti@univ-lyon1.fr

Abstract

The purpose of this work is to devise algorithms to reduce the memory consumption of the vector Preisach model in view of its usage in Finite Element analysis. Four algorithms, which all implement a vector Preisach hysteresis model, are presented and critically compared theoretically and by numerical experiments taken on with two materials and three signals. Several strategies are presented to reduce both the memory occupation and the computational cost of several orders of magnitude.

Introduction

The hysteresis phenomena of the magnetic materials can be modelled using different approaches depending on the scale length of the component taken into account. The magnetic hysteresis at ultra-millimeter scale length, such as the components involved in the electrical machines, power converters, permanent magnets, magnetic recording and magnetic sensors, is in general represented using phenomenological models. About that some of the most used and applied are the Jiles Model [1-4], the Play Model [5-8], the Equivalent Ellipse Model [9] and the Preisach Model [10-12]. The latter one, called also the Classical Scalar Preisach Model, can be generalized for the representation of vector hysteresis to the 2-d and 3-d cases as indicate in a series of previous papers [13-17], hereafter called Vector Hysteresis Model to distinguish it from the Preisach-Mayergoyz model [11] and its improvements [24-26]. This vector approach is based on the definition of a vector mathematical operator, called for convenience here vector hysteron, described in the H-space by a closed and convex critical surface. Each vector hysteron has a unique critical surface, described by a suitable set of parameters, indicated here with the parameter vector $\boldsymbol{\Omega}$. The magnetization state vector of the hysteron can be denoted by the unitary and dimensionless vector $\mathbf{Q}(\boldsymbol{\Omega},\mathbf{H})$. This means that the direction of the unit magnitude magnetization is a single-valued function of the applied magnetic field outside the critical surface and a multivalued function determined by the magnetization history inside the critical surface. For clarity we refer here to the case of two dimensions, where the hysteron critical surface become to a critical curve. In particular we refer to the circular hysteron as described in the figure 1. The components of $\boldsymbol{\Omega}$, i.e. the model parameters, are the components of the interaction field (H_{Ix}, H_{Iy}) that identify the hysteron centre and the value of the parameter u that is the hysteron radius, as described in more detail in the references above mentioned and in the following. The hysterons are

distributed in the H-plane, and their density distribution can be described by a dimensionless function $P(\Omega)$. The rules of this generalized vector model of hysteresis are:

- the normalized component of the magnetization for each hysteron has unit magnitude everywhere;
- for fields inside the critical surface the magnetization is frozen in the direction that it had just before it entered the critical surface, and it remains constant until it exits the critical surface;
- when exiting the critical surface the irreversible magnetization instantly rotates so as to align itself along a new direction, from the hysteron centre to the vertex of the applied magnetic field. This behaviour is corresponding to the Barkhausen jumps that occur in the magnetic materials.
- the total magnetization is the vector sum of the magnetization due to all the vector hysterons.

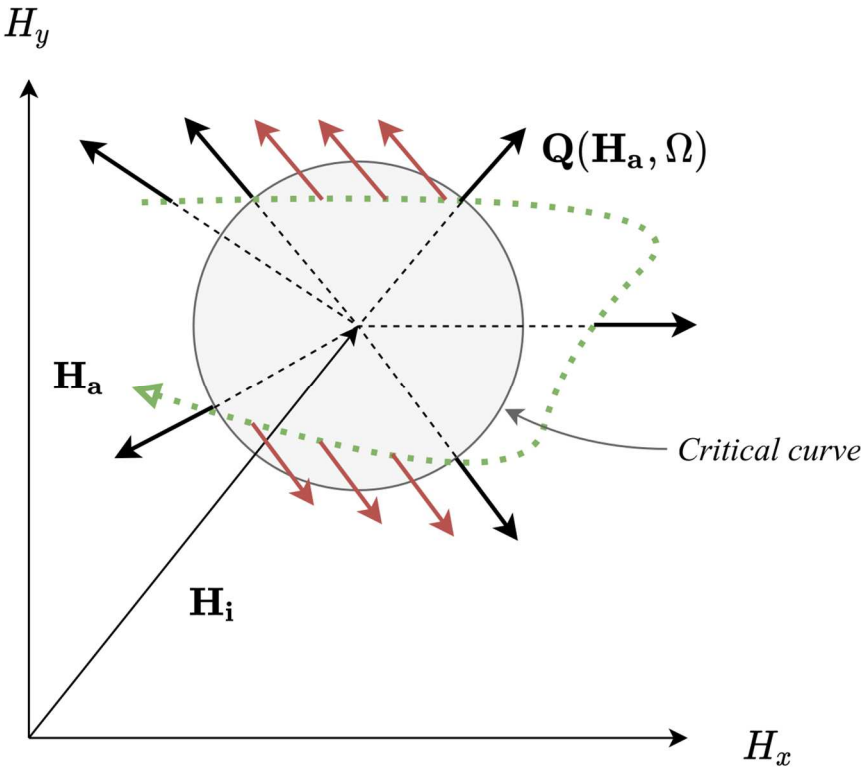

Figure 1. An example in 2-D of hysteron and of the rules of magnetization change with the applied field for a particular applied field $\mathbf{H_a}$ trajectory. $\mathbf{H_i}$ is the center of the hysteron. Frozen unitary magnetization vectors are depicted in red color.

In previous papers [13-19] some general properties of the vector hysterons are shown. In particular we have proved in rigorous mathematical way that is possible define some classes of hysteron where:

- the critical surfaces of the vector hysterons are equipotential surfaces
- the lines of force of the M-field of a vector hysteron are always straight lines.
- the critical surface of the vector hysterons must obey to a necessary and sufficient conditions in order to satisfy the conservative properties of vector fields.

- the critical surface of the vector hysterons must satisfy an additional necessary and sufficient condition for the congruency with the second principle of the thermodynamics.
- any assembly of vector hysterons defined as above obeys to the saturation property, to the losses property, to the deletion and the congruency property.

The generalization of the Preisach method to the representation of magnetic hysteresis in 3-d has proved to be precise, efficient and robust in the reproduction of the state of magnetization of many magnetic materials widely used in many industrial and aerospace applications. However, the use of this methodology involves some disadvantages, which did not allow a full application to the numerical analysis of 3-d electromagnetism problems with the use of Finite Element techniques [28]. Among these disadvantages it is worth mentioning the considerable memory space necessary to take into account the state of each hysteron, which can change according to the magnetic field applied.

In consideration of the fact that the numerical representation of the vector hysteresis, if not appropriately corrected, requires the definition of hundreds of thousands of hysterons in complicated geometries such as those referring to electromagnetic applications in the industrial and aerospace fields mentioned, it appears evident that each method of reducing the number of hysterons or grouping them can have a significant effect on the duration and memory requirement in numerical processing. It has to be mentioned that recent works have been devoted to acceleration of the Preisach-Mayergoyz model by using Everett function [22-23, 27]. However the ideas developed in these works cannot be transposed (at least not straightforwardly) to the Vector Hysteron Model.

In this paper we present a new strategy to reduce the computational resources required to simulate a vector Preisach model, in view of its implementation on Finite Element analysis (FEA). The first purpose of this work is to reduce of several orders of magnitude memory requirements. Unfortunately, the economy in memory resources comes with a proportional increase of the computational time. Hence, the second (but not less important) point which is addressed in this work is the reduction of the computational time.

This article is organized as following. First, the proposed algorithms are presented, and compared with the classical algorithm described in the paper [20] which is extremely greedy in terms of memory occupation. Then two strategies to reduce the computational times are presented: the first one is based on filtering out a significant part of hysterons. The second strategy is based on the generation of reduced models, depending on the applied magnetic field. The proposed algorithms are compared with respect of several signals representative of magnetic materials for electrical machine cores and of magnetic components for power electronics. Conclusions and perspective of future works conclude the article.

Materials and Methods

Hereafter are presented several algorithms which implement the vector Preisach model in a 2D space:

- Basic algorithm: this is a quite standard algorithm which implements Preisach model. The state of each hysterons is stored explicitly;
- Pooled algorithm: this is a variation of the basic algorithm where only the unit polarization of frozen hysterons is stored;

- Memoryless algorithm: in this algorithm, the state of the model is represented by the past and present applied magnetic field;
- Incremental algorithm: this algorithm is a variant of the memoryless algorithm, which is theoretically more computationally efficient and more suitable for further improvements.

It is assumed that critical surfaces of hysterons are circles. For each hysteron, the radius and the center of the crucial surface are denoted respectively by u_i and $\mathbf{H}_i$. The number of hysterons and of computational points (that is, of elements which compose a ferromagnetic region) is indicated respectively by N and M. It can be foreseen that in practical FEA, $N = 10^5$ and $M = 10000$ are realistic values (for instance, see [29, 30] for academic and practical 2d examples, and [31] for a practical 3d example). It is important to keep in mind these orders of magnitudes, in order to analyse the computational cost of these algorithms in view of their application in FEA.

Basic algorithm

In the basic algorithm, the state of each hysteron is represented by its unit polarization $\mathbf{Q}_i$ at any time, and in all computational points. At any time step, for each computational point n and for each hysteron i, the vector $\mathbf{r}_{ni}$ is computed:

$$\mathbf{r}_{ni} = \mathbf{Ha}_n - \mathbf{H}_i \tag{1}$$

where $\mathbf{Ha}_n$ is the magnetic field externally applied in the nth computational point. If $\|\mathbf{r}_{ni}\| > u_i$ or if the hysteron get frozen at this time step (that is, if the hysteron was not frozen in the previous time step and $\|\mathbf{r}_{ni}\| \le u_i$), the value of the unit polarization is updated:

$$\mathbf{Q}_{ni} \leftarrow \frac{\mathbf{r}_{ni}}{\|\mathbf{r}_{ni}\|} \tag{2}$$

Otherwise, if the hysteron is already frozen the unit magnetization is unchanged. Notice that in this case $\mathbf{Q}_{ni}$ has the value, which it had since the hysteron got frozen. In the continuous case, the total polarization in the point n is computed as [32]:

$$\mathbf{J}_n = \alpha \iiint \mathbf{Q}_n(H_{xi}, H_{yi}, u) P(H_{xi}, H_{yi}, u)\, dH_{xi} dH_{yi} du \tag{3}$$

After discretisation, the former equation writes:

$$\mathbf{J}_n = \alpha \sum_{i=1}^{N} \mathbf{Q}_{ni} w_i \tag{4}$$

where w_i is the weight of the i^{th} hysteron defined by $P(\Omega)$, and α is a scaling coefficient corresponding to the saturation polarization. The other relevant quantities are defined as usual:

$$\mathbf{M} = \frac{1}{\mu_0}\mathbf{J} \quad ; \quad \mathbf{B} = \mu_0(\mathbf{H}+\mathbf{M}) = \mu_0\mathbf{H} + \mathbf{J} \tag{5}$$

When this algorithm is used in FEA, the size of the state is of at least MN vectors, in that N vectors have to be stored for each of the M computational points. Just to give an order of magnitude, if two double precision values are required for each vector (that is, 16 bytes), the memory occupied by the set of unit magnetization vectors $\mathbf{Q}_{ni}$ only would be of 16 Gb in our reference case ($N = 10^5$, $M = 10000$). As for the computational time, it is dominated by the time required to upgrade all hysterons in all points, that is $\mathrm{O}(MN)$. To wrap up, the space and time complexity of the basic algorithm are both $\mathrm{O}(MN)$. This algorithm is taken as reference for the algorithms presented hereafter.

Pooled algorithm

The "pooled" algorithm is a variant of the basic algorithm where only the state of frozen hysterons is stored. This algorithm allows an economy of memory, in that the space complexity is $\mathrm{O}(fMN)$, where $f < 1$ is the average fraction of frozen hysterons, which cannot be foreseen in advance. Provided that the extra computational burden to handle the pool of frozen hysterons is negligible, the time complexity is unchanged, that is $\mathrm{O}(MN)$.

Memoryless algorithm

In the "memoryless" algorithm, the state of each computational point is represented by the set of the present and all past values of the applied magnetic field $\mathbf{Ha}_n$ which have been applied to the computational point. At each time step, vector $\mathbf{r}_{ni}$ is computed for each hysteron, and for each computational point (Equation 1). If the hysteron is not frozen, then the unit magnetization $\mathbf{Q}_{ni}$ is computed by using Equation 2. Otherwise, in order to know the unit polarization it is mandatory to go back in time up to the time step when the hysteron got frozen. Finally, the total polarization is computed by using Equation 4.

This algorithm allows a dramatic reduction of the required memory, because for each computational point it is necessary to store only the past values of the applied magnetic field, hence the space complexity is $\mathrm{O}(MT)$ where T is the number of time steps. It can be easily foreseen that in practice $T \gg N$ by several orders of magnitude (for instance, see [29-31] for practical values of *T*), hence this algorithm has a dramatic advantage in terms of memory occupation with respect of the basic algorithm. As for the computational time, it depends on the state of hysterons (frozen / unfrozen). Basically, unfrozen hysterons cost no more than in the basic algorithm, whereas the cost of frozen hysterons is much higher, and increases with the number of time steps. Hence, the time complexity is bounded by $\mathrm{O}(MN(1+fT))$. However, it is evident that the price to pay to reduce the memory occupation is an increase of computational time.

Incremental algorithm

In the "memoryless" algorithm, hysterons with "huge" radius u_i are extremely expensive, on one hand because they are likely to be frozen for most of time steps, and on the other hand

because the computational effort required to come back in time up to the instant when they got frozen (if any) is much higher with respect of "small" hysterons. Moreover, in most of time steps, the algorithm will repeat the same computation, which will provide the same unit magnetization of many previous time steps. The idea behind the "incremental" algorithm is to split the total polarization as the sum of the contribution of frozen and unfrozen hysterons:

$$\mathbf{J}_n = \mathbf{J}_n^{(u)} + \mathbf{J}_n^{(f)} \tag{6}$$

For each time step and for each computational point, only $\mathbf{J}_n^{(f)}$ is stored in the state, and upgraded at any time step. Four cases must be distinguished, depending on the state of the hysteron at the last (= present) and at the second-to-last (= previous) time step:

1. The hysteron is unfrozen, and was already unfrozen at the previous time step: the unit polarization of this hysteron, computed by Equation 2, is added to obtain $\mathbf{J}_n^{(u)}$.
2. The hysteron is frozen, and was already frozen at the previous time step: there is nothing to do, because in this case the contribution of the hysteron is already taken into account by $\mathbf{J}_n^{(f)}$.
3. Transition unfrozen $\rightarrow$ frozen: the unit polarization of the hysteron, computed by Equation 2, is added to $\mathbf{J}_n^{(f)}$.
4. Transition frozen $\rightarrow$ unfrozen: this is the most complex case because the unit polarization of the *hysteron back in time when it got frozen* has to be retrieved, and subtracted from $\mathbf{J}_n^{(f)}$. Then, the present unit polarization of the hysteron is computed by Equation 2 and added to $\mathbf{J}_n^{(u)}$.

One observes that, from the point of view of computational time, hysterons in the case (1)-(4) cost no more than in the basic algorithm. Indeed, hysterons which are and remain frozen (case 2) do cost even less than in the basic algorithm. In particular, huge hysterons which got frozen and unfrozen very seldom has a marginal cost with respect of the memoryless algorithm. Conversely, hysterons which fall in the case (4) require more computational time, but not more than in the case of memoryless algorithm. As for the memory requirement, this algorithm is marginally more expensive than the memoryless algorithm, because for each computational point the vector $\mathbf{J}_n^{(f)}$ has to be stocked, in addition to the present and past values of the applied magnetic field $\mathbf{Ha}_n$.

To wrap up, it is expected that the space complexity of the incremental algorithm is substantially the same as the memoryless algorithm $\mathrm{O}(M(1+T))$, while the time complexity writes $\mathrm{O}(MN(1+f_u T))$, where f_u is the fraction of hysterons which undergo the transition frozen $\rightarrow$ unfrozen at each time step. If $f_u \ll f$, then the time complexity of the incremental algorithm should be intermediate between the basic and the memoryless algorithm. In this case, the incremental algorithm is the best candidate to replace the basic algorithm in FEA. Conversely, if at any time step the fraction of frozen hysterons f is low with respect of the number of hysterons which get unfrozen ($f_u > f$), the memoryless or even the pooled algorithms could have better performances.

To summarize, the time and space complexity of the four algorithms introduced beforehand are summarized in table 1. One observes that the complexity depends upon some parameters (namely, the number of time steps T, the fraction of frozen hysterons f and the fraction of hysterons which got unfrozen f_u) which are impossible to predict with no *a priori* information, and which depends on the simulated signals and on the set of hysterons which model magnetic materials.

It is important to observe that space complexity of the basic and pooled algorithms scales with the number of hysterons N, whereas the one of memoryless and incremental algorithms scales with the number of time steps T. Hence, from the point of view of memory occupation, these algorithms are expected to behave in a very different way. In particular, the memoryless and incremental algorithms are foreseen to be more suitable for FEA, when a large number of elements have to be considered.

Table 1: Time and space complexity of algorithms.

Algorithm	Basic	Pooled	Memoryless	Incremental
Time complexity	$\mathrm{O}(MN)$	$\mathrm{O}(MN)$	$\mathrm{O}(MN(1+fT))$	$\mathrm{O}(MN(1+f_uT))$
Space complexity	$\mathrm{O}(MN)$	$\mathrm{O}(fMN)$	$\mathrm{O}(MT)$	$\mathrm{O}(M(1+T))$

Magnetic materials used in simulations

The algorithms have been tested with two fictive isotropic magnetic materials (hereafter named material #1 and material #2, or simply #1 and #2). These materials are characterized by N_1 = 134000 and N_2 = 150000 hysterons respectively. The scalar magnetization loops for these two materials are depicted in Figure 2. Their magnetic behaviour is very similar to the electrical steel FeSi non oriented grain, with two different grade of differential magnetic permeability, lower for the #1 and higher for the #2. At present time, moving is not implemented in our algorithms; hence it is not possible to simulate realistic anisotropic materials. The distribution $P(\Omega)$ for these materials is depicted in Figure 3.

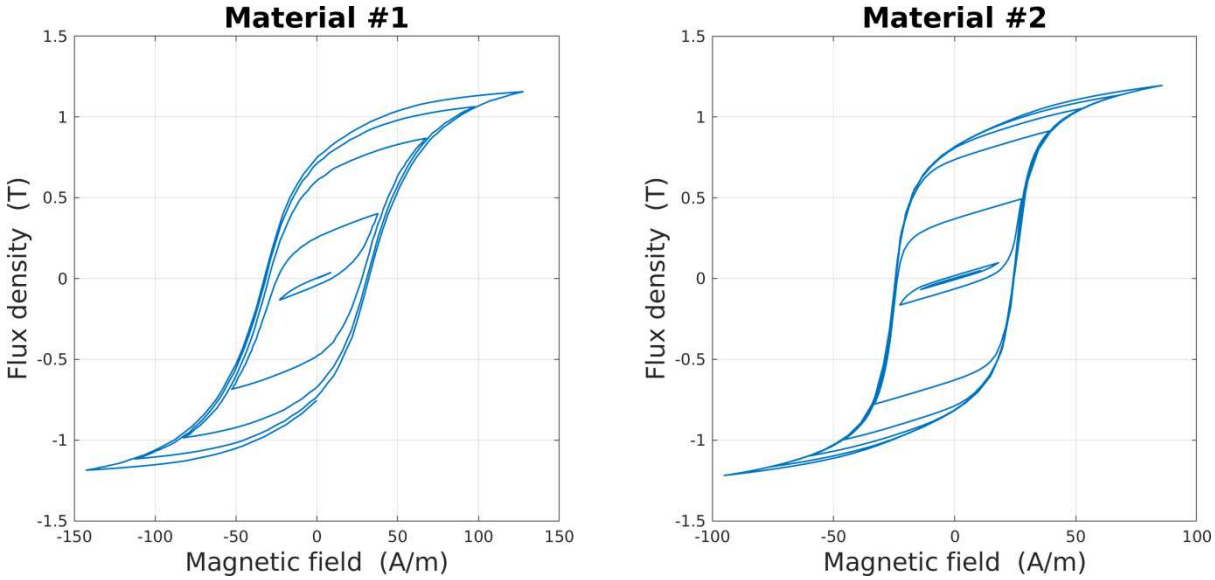

Figure 2. Scalar magnetizing loops for materials #1 and #2.

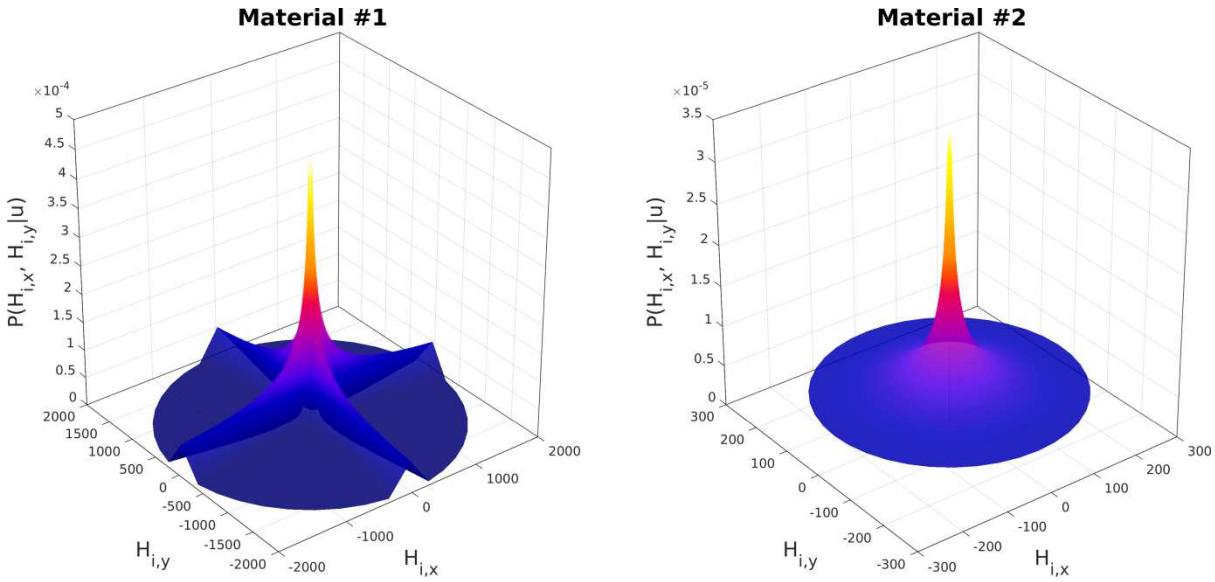

Figure 3. Distribution $P(\Omega)$ for the materials #1 and #2 for a fixed value of the radius of hysterons u.

Simplification of the set of hysterons

The number of hysterons in vector Preisach models is generally very high (of the order of 10^3 – 10^5 hysterons). However, most of hysterons have a very small weight. In Figure 4 (left) it is depicted the histogram of the weights of hysterons for the material #1 used in this work. It can be observed that a huge number of hysterons have a very small weight, and hence their contribution to the total magnetization is small. For instance, in Figure 4 (right) it is depicted the cumulate distribution of the weights of hysterons with respect of the fraction of hysterons, in the case of material #1. It can be observed that the 86 % of hysterons with the smallest weights taken all together contribute to only 2 % of the overall weight.

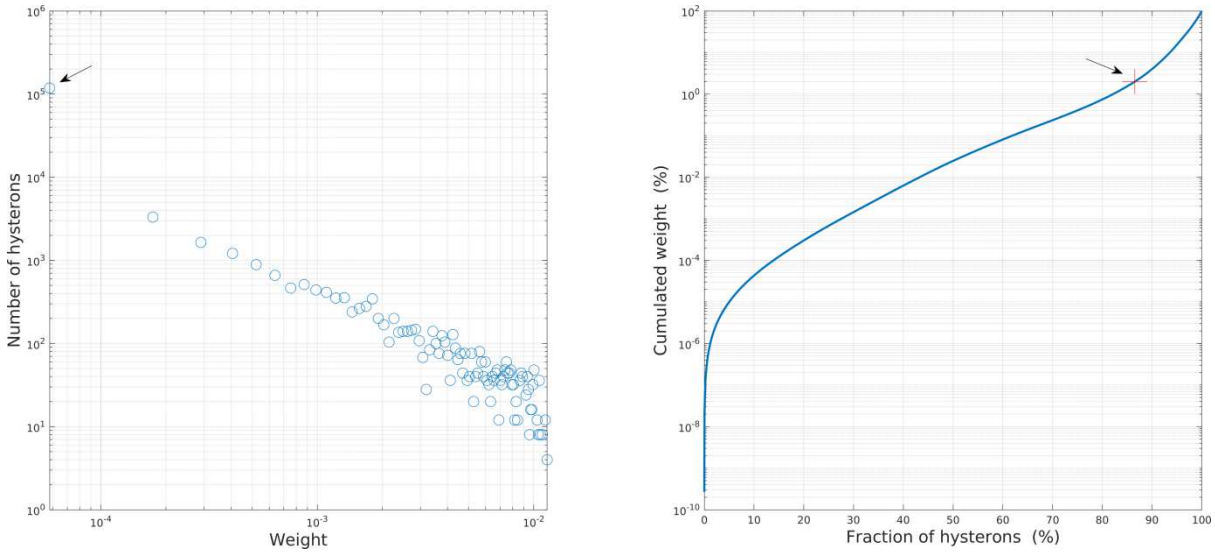

Figure 4. Left: histogram of the weights of hysterons of material #1. Right: cumulated distribution of the weights of hysterons. The arrow indicates the point corresponding to the threshold weight w^* for p = 2 % (right), and the class to which hysterons with weight $w<w^*$ belong (left).

In order to simplify the set of hysterons, let's define "threshold" weight w^* such that:

$$\sum_{w_i<w^*} w_i = p \tag{7}$$

where p is the fraction of hysterons which will be discarded. Let $\mathbf{J}^*$ be the polarization computed by trunking the sum of Equation 4 so as to neglect hysterons, the weight of which is smaller than w^*:

$$\mathbf{J}^* = \alpha \sum_{w_i \geq w^*} \mathbf{Q}_i w_i \tag{8}$$

The maximal absolute error on the approximated magnetization $\mathbf{J}^*$ will be at most αp, which is much smaller than usual experimental error:

$$\left\| \mathbf{J} - \mathbf{J}^* \right\| = \alpha \left\| \sum_{w_i<w^*} \mathbf{Q}_i w_i \right\| \leq \alpha \sum_{w_i<w^*} \left\| \mathbf{Q}_i \right\| w_i = \alpha p \tag{9}$$

A similar bound can be devised for the relative error with respect of the maximum value of the polarization:

$$e_{max} = \frac{\max \left\| \mathbf{J} - \mathbf{J}^* \right\|}{\max \left\| \mathbf{J} \right\|} \leq \frac{\alpha \sum_{w_i<w^*} \left\| \mathbf{Q}_i \right\| w_i}{\alpha \sum \left\| \mathbf{Q}_i \right\| w_i} = p \tag{10}$$

This bound is sharp, and the equality holds for very high magnetic fields, where all unit polarizations $\mathbf{Q}_i$ are practically aligned. Notice that it is impossible to devise a practical error bound for the relative error on the polarization itself (that is, for $\left\| \mathbf{J} - \mathbf{J}^* \right\| / \left\| \mathbf{J} \right\|$).

One observes from Equation 9 that by simply truncating the sum in Equation 8 so as to neglect hysterons with the lowest weight, the saturation polarization is reduced proportionally. This gives rise to the highest error when the material is closed to saturation, which is an undesirable behaviour (Figure 5). A possible mitigation strategy is to rescale the prefactor α in Equation 8 so as to conserve the maximum polarization, that is:

$$\alpha^* = \frac{\alpha}{\sum_{w_i \geq w^*} w_i} \quad ; \quad \mathbf{J}^* = \alpha^* \sum_{w_i \geq w^*} \mathbf{Q}_i w_i \tag{11}$$

It is observed that most of removed hysterons have a large radius. In the case of material #1 the average radius of hysterons $\{u_i\}$ is lowered from 1319 A/m to 89.7 A/m for the simplified set (with p = 2 %). The case of material #2 is similar: under the same hypothesis, the average radius is lowered from 180.6 A/m to 28 A/m. When using a simplified set of hysterons it can be foreseen that the fractions f and f_u will be lower with respect of the original set. Notice that this contributes to reduce the computational complexity for the memoryless and

incremental algorithms (Table 1). Similar considerations apply also to the position of hysterons $\|\mathbf{H}_i\|$, as it can be easily understood by looking at Figure 3.

In the case of material #1, by removing the 86 % smallest hysterons, it is possible to reduce of 86 % the computational cost and the price to pay for this approximation is an error of at most 2 %. The outcome with material #2 is similar: by removing the 73 % smallest hysterons contribute to only 2 % of the overall weight. Of course the amount of the gain depends strongly on the material, and on how it has been identified. Nevertheless, this simple procedure provides an effective and general strategy to reduce the computational cost of Preisach model, whatever the implemented algorithm.

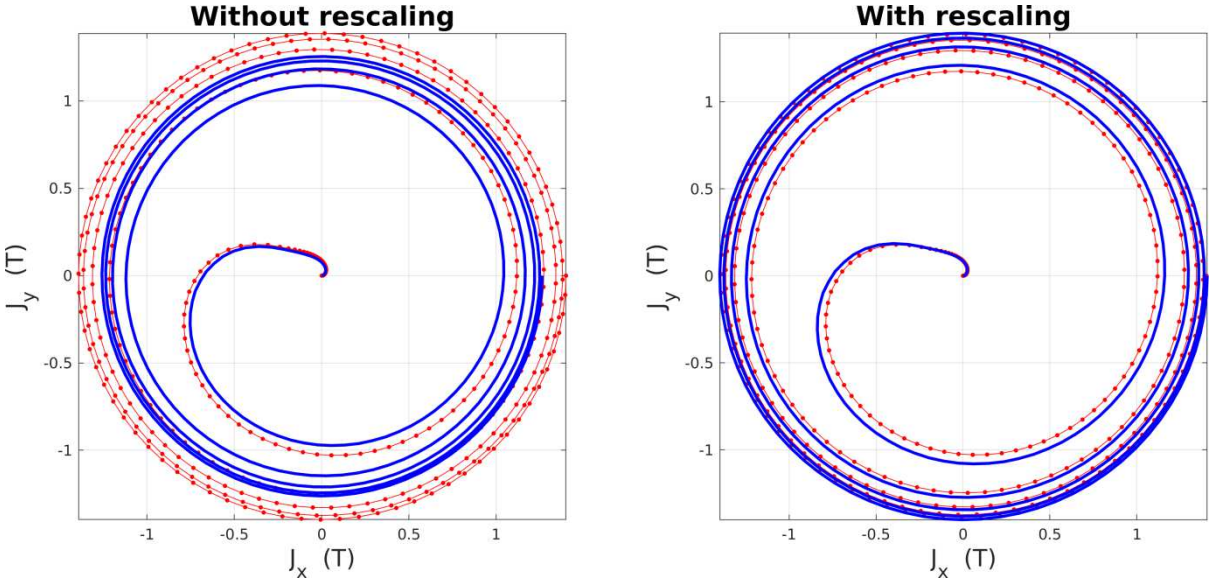

Figure 5. Polarization simulated with a simplified model of material (material #2, p = 10 %) without rescaling (left, Equation 8) and with rescaling (right, Equation 11). Dotted line = reference, simulated with the original, not simplified model.

Generation of reduced models of the material

Even by using the simplification above-mentioned strategy, the number of hysterons remains very high. If it were possible to further reduce the number of hysterons which have to be handled at any time, the computational cost would be reduced proportionally. Hereafter is exposed a strategy based on the creation of reduced models of the material, which are valid while **Ha** lies in a certain neighbourhood of the **H**-plane. This strategy achieves the objective (of reducing the computational cost) at the cost of a moderate approximation, and eventually a few additional computations which can be run off-line. The strategy will be exposed by making reference to the incremental algorithm, but in principle it could be applied also to other algorithms.

The idea is the following: let $\mathrm{B}(\mathbf{Ha}_0,\rho)=\{\mathbf{h}:\|\mathbf{h}-\mathbf{Ha}_0\|<\rho\}$ be a ball of radius ρ centred in a certain value of the applied magnetic field $\mathbf{Ha}_0$, and assume that $\mathbf{Ha}\in\mathrm{B}(\mathbf{Ha}_0,\rho)$. Under this condition, a reduced set of hysterons can be used in the computation, instead of the full set of hysterons. For each domain of validity $\mathrm{B}(\mathbf{Ha}_0,\rho)$, the becoming of each hysteron can be one of the following (Figure 6a):

i. hysterons which are "far enough" from the domain of validity are clustered together to form a tiny subset of N_C heavyweight hysterons,

ii. hysterons which may get frozen / unfrozen, or which are simply too close to the domain of validity are not modified,

iii. hysterons which are frozen, and will remain frozen $\forall \mathbf{Ha} \in \mathrm{B}(\mathbf{Ha}_0, \rho)$ will be removed from the set of hysterons.

The procedure to create reduced models is controlled by two parameters, the signification of which will be clarified hereafter:

- N_C = number of clusters (= heavyweight hysterons),
- $h_{min} > \rho$ = threshold distance for clustering.

Let $r_i = \left\| \mathbf{H}_i - \mathbf{Ha} \right\|$ the distance between the centre of ith hysteron and the applied magnetic field. All hysterons which fulfil the condition:

$$u_i > r_i + \rho \tag{12}$$

are removed, because they are (and remain) frozen $\forall \mathbf{Ha} \in \mathrm{B}(\mathbf{Ha}_0, \rho)$, and hence they fall in the case 2 of the incremental algorithm. We recall that with the incremental algorithm, hysterons which are and remain frozen during a time step are accounted by the term $\mathbf{J}_n^{(f)}$, hence they give no contribution until they get defrozen. All hysterons which fulfil the following condition:

$$r_i > u_i + h_{min} \tag{13}$$

are clustered together into N_C new heavyweight hysterons. The rationale is that "far" hysterons are necessarily unfrozen, and it is not necessary to take into account all of them individually. Instead, they are taken into account collectively into a N_C hysterons, basing on their unit polarization, computed with respect of the centre of the validity domain $\mathbf{Ha}_0$ (Figure 6). In this work, clustering is performed by using the k-means algorithm [21], but other clustering algorithms could fit as well.

For each cluster C, the original hysterons are replaced by a single heavyweight hysteron. A desirable property of this new hysteron would be that it gives exactly the same contribution as the set of clustered hysterons when $\mathbf{Ha} = \mathbf{Ha}_0$, that is:

$$\sum_{i \in \mathrm{C}} w_i \mathbf{Q}_i = w_{HW} \mathbf{Q}_{HW} \quad \Leftrightarrow \quad \mathbf{Q}_{HW} = \frac{1}{w_{HW}} \sum_{i \in \mathrm{C}} w_i \mathbf{Q}_i \tag{14}$$

where w_{HW} and $\mathbf{Q}_{HW}$ are respectively the weight and the unit polarization of the heavyweight hysteron for $\mathbf{Ha} = \mathbf{Ha}_0$. The weight w_{HW} of the heavyweight hysteron is the sum of the weights of clustered hysterons:

$$w_{HW} = \sum_{i \in \mathrm{C}} w_i \tag{15}$$

It is observed that Equation 14 is verified with excellent approximation if the centre $\mathbf{H}_{HW}$ of the heavyweight hysteron is set to the barycentre of the original hysterons. In fact, Equation 14 writes:

$$\mathbf{Q}_{HW} = \frac{\mathbf{Ha}_0 - \mathbf{H}_{HW}}{\left\|\mathbf{Ha}_0 - \mathbf{H}_{HW}\right\|} = \frac{\sum_{i\in C} w_i \dfrac{\mathbf{Ha}_0 - \mathbf{H}_i}{\left\|\mathbf{Ha}_0 - \mathbf{H}_i\right\|}}{\sum_{i\in C} w_i} \tag{16}$$

For the sake of simplicity, and without loss of generality, assume that $\mathbf{Ha}_0 = 0$; then Equation 8 writes:

$$\mathbf{H}_{HW} = \frac{\sum_{i\in C} w_i \mathbf{H}_i \dfrac{\left\|\mathbf{H}_{HW}\right\|}{\left\|\mathbf{H}_i\right\|}}{\sum_{i\in C} w_i} \approx \frac{\sum_{i\in C} w_i \mathbf{H}_i}{\sum_{i\in C} w_i} \tag{17}$$

Finally, the radius of the new hysteron plays no role because clustered hysterons are unfrozen by construction.

The threshold distance $h_{min} > \rho$ controls the approximation error, by avoiding to cluster unfrozen hysterons which are "too close" to the validity domain. The rationale is that when the applied field **Ha** lies in the validity domain, the variation of the unit polarization $\mathbf{Q}_i$ of any hysteron is bounded by (Figure 6b):

$$\left\|\delta\mathbf{Q}_i\right\| < 2\sin\gamma = \frac{2\rho}{h_{min}} \tag{18}$$

In practice one would like to cluster as many hysterons as possible (that is, to select a value of h_{min} close to ρ), but on the other hand small values of h_{min} could compromise the accuracy of the approximation. The other parameter which has an influence on the accuracy is of course the number of clusters N_C: the bigger N_C, the higher the accuracy.

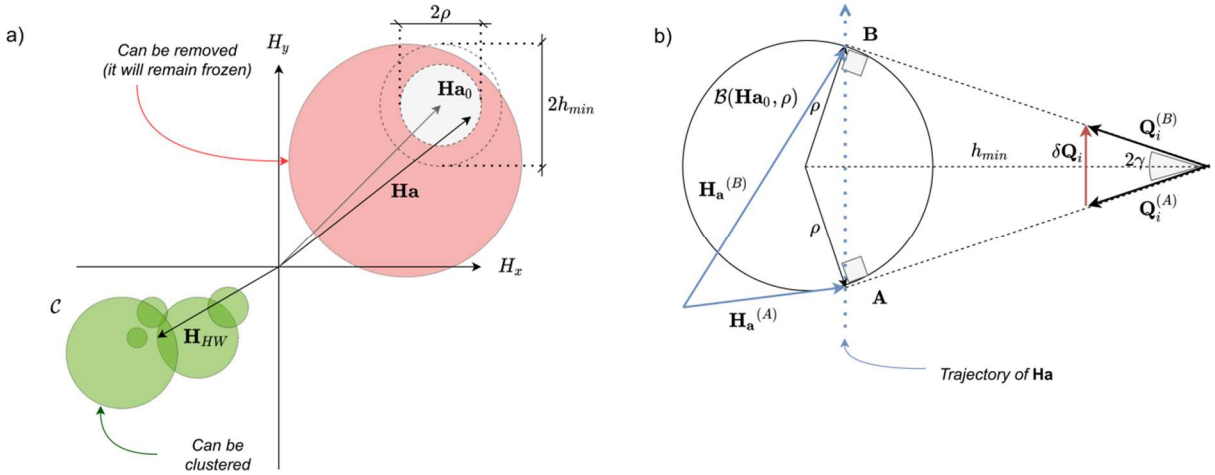

Figure 6. a) Sketch of the reduction algorithm. The red hysteron, which is and will remain frozen for any **Ha** within the validity domain, is removed (case iii). Green hysterons, which have similar unit magnetization, are clustered into a new heavyweight hysteron (case i). The remaining hysterons are not modified (case ii). b) Maximum variation of $\delta\mathbf{Q}_i$ when the applied magnetic field $\mathbf{H_a}$ lies inside the validity domain, which happens when trajectory of the applied magnetic field moves from $\mathbf{H_a}^{(A)}$ to $\mathbf{H_a}^{(B)}$.

Implementation

All those algorithms have been implemented in Matlab/Octave language[1]. Needless to say, this language can eventually provide high performances, provided that computations are vectorised. Vectorization is easy in the case of the basic algorithm, whereas it appears to be quite difficult – if not impossible – for other algorithms, in particular for the incremental algorithm. For this unfortunate reason, precautions are mandatory when measuring time complexity. In this work, time complexity has been evaluated by using the two following quantitative indicators:

- The number of computations of unit magnetization (Equations 1 and 2) is tracked, in order to get an estimate of the number of elementary operations executed by each algorithm,
- In computer programs used to measure execution time, vectorization has been purposely avoided, so as to achieve a fair comparison between algorithms. This precaution is key: for instance, in one of our tests the execution times for the basic algorithm in the case of vectorized and not vectorized codes are respectively 0.3 and 4.8 seconds, whereas the number of elementary operations is strictly identical.

Nevertheless, in our opinion the most reliable indicator of time complexity is from far the number of execution of elementary operations. Hereafter, execution times are provided only for the sake of completeness, but data is interpreted basing on the number of elementary operations only.

Several strategies can be devised to handle model reduction. A whole set of reduced models can be generated off-line (once for each material), or on-the-fly during simulations. For a given pool of reduced models, the search of the most appropriate model for each computational point can be done in several ways (linear search, oct-tree search, etc.). By the way, some points belong to more than a single validity domain, hence several reduced models could be used. This could help to mitigate the discontinuity which happens when a point "jumps" from a validity domain to another. In this work we have implemented a simple strategy, based on a dynamical set of reduced models which is populated during the simulation. For each computational point, a single reduced model is employed, and it is selected by linear search.

Similarly, the strategy to handle the "history" of the material can be implemented in several ways, and it is prone to optimization. Notice that, in view of utilisation of Preisach model in FEA, one is obliged to compute and store somewhere the past values of the magnetic field. However, it is not guaranteed that Finite Element software interfaces allow to look back for the past values of the magnetic field during the resolution; and whenever this could be possible, this is likely to come with an additional computational cost. In other words: in principle computing and storing the past values of the magnetic field during FEA does not increases the overall computational cost, but in practice retrieving this information by using existing Finite Element software could be costly, or complicate (if not impossible).
In this work, the magnetic field at all the time steps, and for all computational points, is stocked within the software component which models the material, so as to avoid the complexity of interfacing with Finite Element software. The price to pay is of course a duplication of data, because the past magnetic field in magnetic materials has to be stocked

[1] More precisely, programs have been developed by using Matlab 2020b on a standard laptop running Linux.

twice (once in the component which models magnetic materials, and the other on the FEA side). The search back in time for the unit magnetization of frozen hysterons is performed by linear search.

Results and Discussion

Simulated signals

We performed several tests by using as excitation magnetic field $\mathbf{H}_a$ the following signals:

1. Spiral: the magnitude of the magnetic field increases linearly, while its orientation rotates at a constant rate. This highlights the vector behaviour of the material,
2. Periodic signal with 3rd harmonic: this signal is representative of the kind of signals which can be encountered in some real electrical appliances, notably in the T-joints of transformers,
3. Pseudo-scalar signal: this signal excites the material in several directions, but in each direction the excitation is delivered in a "scalar fashion", that is with no modification of the direction of the field.

Hereafter these signals will be denoted "spiral", "harmonics" and "scalar" respectively. For each signal, the magnetic field $\mathbf{H}_a$ and the computed polarization $\mathbf{J}$ (all algorithms provide exactly the same result) are depicted in Figure 7 for the material #1. Each signal is discretized in $T = 400$ time steps.

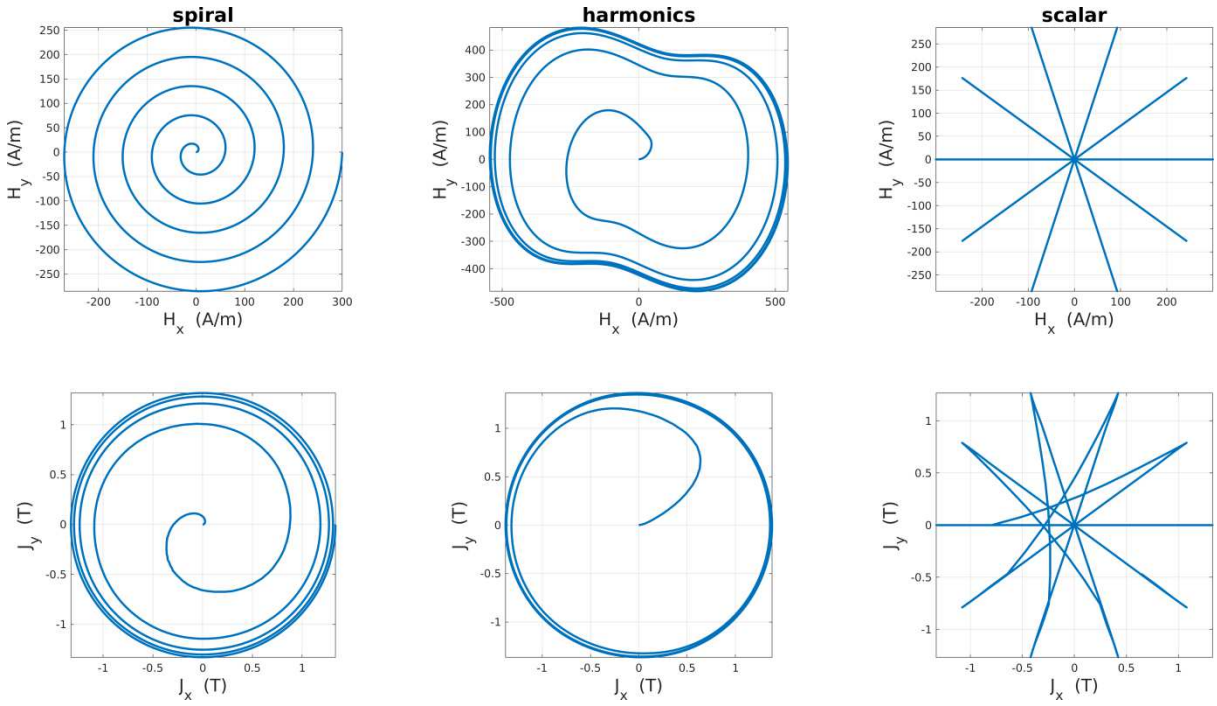

Figure 7. Excitation magnetic field $\mathbf{H}_a$ and the corresponding polarization $\mathbf{J}$ simulated with material #1 for the signals "spiral", "harmonics" and "scalar".

Comparison of algorithms

The time and space complexity of the four algorithms introduced have been measured "experimentally" by simulating the excitation of an isotropic magnetic material by the three

signals depicted in Figure 7. Simulations have been performed on a single computational point by using materials #1 and #2. For all simulations, the number T_{OP} of elementary operation, the execution time T_{CPU} and the required memory T_{MEM} have been tracked and reported in Table 2. We stress that the reported computational times are not representative of a "true" implementation, and are provided for completeness only. In these simulations the materials are simulated "as such", that is neither simplification nor reduction strategies are employed.

Table 2: Statistics of the simulations with several excitation signals (M = 10^6 elementary operations). No simplification / reduction are used. Symbols #1 and #2 indicate the material used in simulations.

Algorithm			Basic	Pooled	Memoryless	Incremental
"spiral"						
Time complexity	T_{op}	#1	53.7 M	53.7 M	5841 M	111 M
		#2	60.2 M	60.2 M	3701 M	133 M
	T_{cpu}	#1	84.7 sec	1931 sec	522 sec	90 sec
		#2	66.0 sec	1345 sec	358 sec	260 sec
Space complexity	T_{mem}	#1	2.27 Mb	1.75 Mb	1.61 kb	2.3 kb
		#2	2.55 Mb	0.89 Mb	1.77 kb	2.5 kb
"harmonic"						
Time complexity	T_{op}	#1	53.7 M	53.7 M	4949 M	112 M
		#2	60.2 M	60.2 M	640 M	128 M
	T_{cpu}	#1	77.0 sec	1561 sec	464 sec	98 sec
		#2	29.7 sec	337 sec	144 sec	207 sec
Space complexity	T_{mem}	#1	2.27 Mb	1.61 Mb	1.61 kb	2.3 kb
		#2	2.55 Mb	0.24 Mb	1.77 kb	2.5 kb
"scalar"						
Time complexity	T_{op}	#1	53.7 M	53.7 M	5580 M	111 M
		#2	60.2 M	60.2 M	2586 M	130 M
	T_{cpu}	#1	83 sec	1852 sec	508 sec	85 sec
		#2	58 sec	1120 sec	285 sec	227 sec
Space complexity	T_{mem}	#1	2.27 Mb	2.01 Mb	1.61 kb	2.3 kb
		#2	2.55 Mb	2.34 Mb	1.77 kb	2.5 kb

Space complexity: the difference in memory occupation between the first two algorithms (basic and pooled) and the last two ones is striking (memoryless and incremental). The

difference is of the same order of magnitude of the ratio between the number of hysterons and the number of time steps. For instance, for material #1 one has:

$$\text{Material \#1}: \quad \frac{N}{T} = \frac{134000}{400} = 335 \quad \sim \quad 987 = \frac{2.27\ \text{Mb}}{2.3\ \text{kb}} \tag{19}$$

Conversely to the other algorithms, the memory occupation of the pooled algorithm is not a constant value, because it depends on the fraction f of frozen hysterons, which varies with the particular time step, the signal and of course the material (Figure 8). The occupied memory T_{mem} reported in Table 2 have been tracked at the last time step, but they are well representative of the general trend, apart for the signal "scalar". With the material #1 the average fraction f of frozen hysterons is of about 50- to 60- % at any iteration, and for all signals. Conversely, in the case of material #2 the fraction f of frozen hysterons spans in a much broader range $[0.05\ ;\ 0.65]$. It is observed that higher excitation field values are correlated with smaller fraction of frozen hysterons, whereas the higher value is generally found in the virgin state.

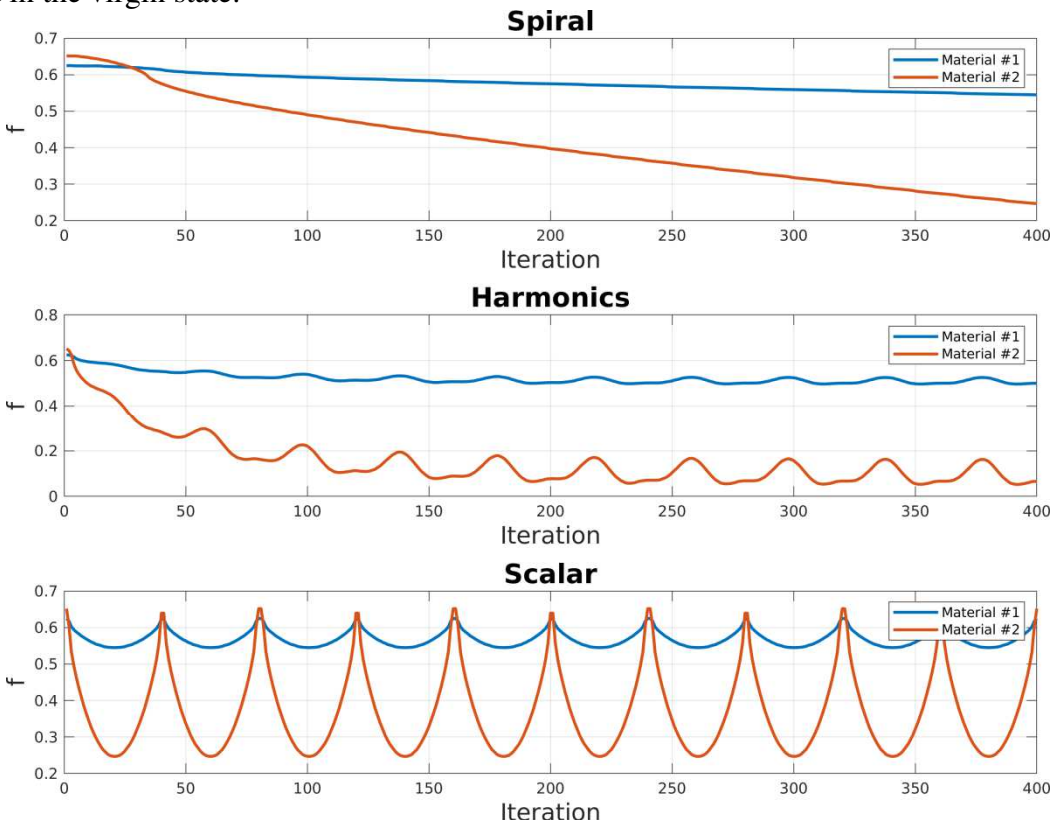

Figure 8. Fraction of frozen hysterons as a function of the iteration for the signals "spiral", "harmonics" and "scalar".

Time complexity: the number of elementary operations for the basic and the pooled methods is identical. Even by taking into account the additional burden of handling the pool of frozen hysterons, these two algorithms have fundamentally the same time complexity. The huge difference in the measured computational time reported in Table 2 is only a matter of implementation: indeed when both algorithms are vectorised, they exhibit similar computational times[2]. The much larger number of elementary operations required by the

[2] More precisely, the maximum measured execution time for the vectorized versions of basic and pooled algorithms are respectively 2.4 sec and 3.2 sec for material #1.

memoryless algorithm is representative of the fraction of frozen hysterons (Figure 8). Frozen hysterons are very expensive in terms of computational time, because the memoryless needs to go back in time to retrieve the time step when they got frozen. Conversely, the incremental algorithm is competitive, in that its computational time is of the same order of magnitude of the basic algorithm. This difference is due to the fact that, even if about 60 % of hysterons are frozen at any time step, only a small fraction of them undergo the transition frozen $\rightarrow$ unfrozen. The huge difference in the number of operations T_{op} between the memoryless and incremental algorithms confirm the hypothesis that in general $f_u \ll f$. However, it must be pointed out that the material and the signal have both a strong influence; for instance, it is observed that the incremental algorithm over the memoryless one is more pronounced for material #1 than for material #2.

To summarize, the theoretical predictions on the time and space complexity are supported by experimental data. The pooled algorithm has a moderate advantage over the basic algorithm in terms of space complexity, and the time complexity is practically the same for these two algorithms. Memoryless and incremental algorithms have both a huge advantage from the standpoint of space complexity, but from the standpoint of time complexity the incremental algorithm seems to be more competitive than the memoryless algorithm.

Influence of the simplification of the set of hysterons

In order to analyse the effect of simplification of the set of hysterons, we repeated the simulations by truncating the set of hysterons so as to discard respectively 1 %, 2 %, 5 % and 10% of the original set of hysterons. The results are analysed in terms of accuracy and from the standpoint of time and space complexity.

As for the accuracy, two indicators e_{max} and e_{rel} have been evaluated:

$$e_{max} = \frac{\max \left\| \mathbf{J}^* - \mathbf{J} \right\|}{\max \left\| \mathbf{J} \right\|} \times 100\ \% = \frac{\max \left\| \mathbf{M}^* - \mathbf{M} \right\|}{\max \left\| \mathbf{M} \right\|} \times 100\ \% \tag{20}$$

$$e_{rel} = \max_{\|\mathbf{M}\| \geq 1\ \mathrm{A/m}} \left(\frac{\left\| \mathbf{M}^* - \mathbf{M} \right\|}{\left\| \mathbf{M} \right\|} \right) \times 100\ \% \tag{21}$$

where $\mathbf{J}$ is the polarization computed with the original set of hysterons, whereas $\mathbf{J}^*$ is computed by using a simplified set of hysterons (similar definitions hold for $\mathbf{M}$ and $\mathbf{M}^*$). Both of all are relative errors: e_{max} is normalized with respect of the maximum value of the magnetization, whereas e_{rel} is a "pure" relative error where small values have been discarded so as to get rid of numerical noise (the threshold value $\|\mathbf{M}\| \geq 1$ A/m has been chosen arbitrarily). The results obtained with rescaling (Equation 11) and without rescaling (Equation 8) are summarized in Table 3 (see also Figure 5).

Accuracy: it can be observed that the theoretical prediction of the error bound for e_{max} is verified (Equation 10). In particular, Equation 10 holds sharply as long as no rescaling is applied, while an improved accuracy is observed when the rescaling is used; the higher the value of *p*, the higher the improvement in the accuracy. However, one must keep in mind that the purpose of rescaling is to conserve the maximum polarization of the material: hence an eventual improvement obtained by using rescaling depends on the material and on the

excitation signal. If the material is going to be saturated, an improved accuracy for high fields can be foreseen. Otherwise, the effectiveness of the rescaling cannot be predicted; in this case, rescaling may even degrade the accuracy. As anticipated beforehand, it is not possible to provide a theoretical bound for the relative error e_{rel}, which is by intrinsically higher than e_{max}.

Table 3: Number of remaining hysterons and error obtained when using simplified sets of hysterons with rescaling (without rescaling). Symbols #1 and #2 indicate the material used for the corresponding line of the table.

p		1 %	2 %	5 %	10 %
Nb. of hysterons	#1	23888	18033	12129	8614
	#2	50205	41044	30996	24266
			"spiral"		
e_{max}	#1	0.83 % (0.83 %)	1.5 % (1.5 %)	3.5 % (3.5 %)	6.0 % (6.0 %)
	#2	0.57 % (0.93 %)	1.0 % (1.9 %)	2.2 % (4.9 %)	4.0 % (9.7 %)
e_{rel}	#1	0.94 % (0.95 %)	1.8 % (1.8 %)	4.2 % (4.3 %)	7.4 % (7.6 %)
	#2	0.77 % (1.45 %)	1.4 % (2.9 %)	3.2 % (7.1 %)	6.2 % (13 %)
			"harmonic"		
e_{max}	#1	0.83 % (0.80 %)	1.5 % (1.5 %)	3.3 % (3.2 %)	5.6 % (5.6 %)
	#2	0.56 % (1.00 %)	0.99 % (2.0 %)	2.1 % (5.0 %)	3.8 % (9.9 %)
e_{rel}	#1	0.94 % (0.95 %)	1.8 % (1.7 %)	4.2 % (4.4 %)	7.4 % (7.5 %)
	#2	0.77 % (1.5 %)	1.4 % (2.7 %)	3.2 % (7.1 %)	6.2 % (13 %)
			"scalar"		
e_{max}	#1	0.85 % (0.21 %)	1.6 % (0.67 %)	4.1 % (2.9 %)	7.8 % (7.6 %)
	#2	0.90 % (0.92 %)	1.5 % (1.9 %)	3.2 % (4.8 %)	5.5 % (9.7 %)
e_{rel}	#1	1.2 % (0.23 %)	1.9 % (1.1 %)	5.0 % (8.0 %)	9.6 % (22 %)
	#2	1.7 % (2.2 %)	2.6 % (3.7 %)	5.2 % (6.4 %)	9.2 % (10 %)

Computational cost: as illustrated in Figure 9, the number of hysterons, and hence the computational cost, can be greatly reduced by neglecting even a small fraction p of the total weight. The total number T_{OP} of elementary operations, and the occupied memory T_{MEM} (at the last iteration only) for the different signals and algorithms are reported in Table 4 (material #1) and Table 5 (material #2).

Table 4: Computational cost when using simplified sets of hysterons (material #1). T_{op} = number of operations (M = 10^6 elementary operations), T_{mem} = occupied memory.

Algorithm	*p*	Basic	Pooled	Memoryless	Incremental
			"spiral"		
T_{op}	0 %	53.7 M	53.7 M	5841 M	111 M
	1 %	9.6 M	9.6 M	375 M	20.6 M
	2 %	7.2 M	7.2 M	184 M	15.6 M
	5 %	4.9 M	4.9 M	49 M	10 M
	10 %	3.5 M	3.5 M	19 M	7 M
T_{mem}	0 %	2.27 Mb	1.75 Mb	1.61 kb	2.3 kb
	1 %	408 kb	85 kb	1.61 kb	2.3 kb
	2 %	308 kb	32 kb	1.61 kb	2.3 kb
	5 %	208 kb	3.7 kb	1.61 kb	2.3 kb
	10 %	148 kb	3.0 kb	1.61 kb	2.3 kb
			"harmonic"		
T_{op}	0 %	53.7 M	53.7 M	4949 M	112 M
	1 %	9.6 M	9.6 M	102 M	20 M
	2 %	7.2 M	7.2 M	14 M	15 M
	5 %	4.9 M	4.9 M	5.6 M	10 M
	10 %	3.5 M	3.5 M	3.8 M	7.0 M
T_{mem}	0 %	2.27 Mb	1.61 Mb	1.61 kb	2.3 kb
	1 %	408 kb	32 kb	1.61 kb	2.3 kb
	2 %	308 kb	3.6 kb	1.61 kb	2.3 kb
	5 %	208 kb	2.5 kb	1.61 kb	2.3 kb
	10 %	148 kb	2.3 kb	1.61 kb	2.3 kb
			"scalar"		
T_{op}	0 %	53.7 M	53.7 M	5580 Mb	111 M
	1 %	9.6 M	9.6 M	254 M	34 M
	2 %	7.2 M	7.2 M	89 M	26 M
	5 %	4.9 M	4.9 M	7.5 M	10 M
	10 %	3.5 M	3.5 M	4.4 M	7.1 M
T_{mem}	0 %	2.27 Mb	2.01 Mb	1.61 kb	2.3 kb
	1 %	408 kb	289 kb	1.61 kb	2.3 kb
	2 %	308 kb	209 kb	1.61 kb	2.3 kb
	5 %	208 kb	141 kb	1.61 kb	2.3 kb

	10 %	148 kb	103 kb	1.61 kb	2.3 kb

Table 5: Computational cost when using simplified sets of hysterons (material #2). T_{op} = number of operations (M = 10^6 elementary operations), T_{mem} = occupied memory.

Algorithm	*p*	Basic	Pooled	Memoryless	Incremental
			"spiral"		
T_{op}	0 %	60.1 M	60.2 M	3701 M	133 M
	1 %	20.1 M	20.1 M	48.8 M	41.4 M
	2 %	16.5 M	16.5 M	32.4 M	33.7 M
	5 %	12.4 M	12.4 M	22.0 M	25.4 M
	10 %	9.7 M	9.7 M	16.7 M	19.9 M
T_{mem}	0 %	2.55 Mb	0.89 Mb	1.77 kb	2.5 kb
	1 %	855 kb	85.0 kb	1.77 kb	2.5 kb
	2 %	700 kb	2.3 kb	1.77 kb	2.5 kb
	5 %	529 kb	2.3 kb	1.77 kb	2.5 kb
	10 %	415 kb	2.3 kb	1.77 kb	2.5 kb
			"harmonic"		
T_{op}	0 %	60.1 M	60.2 M	640 M	128 M
	1 %	20.1 M	20.1 M	20.7 M	40.4 M
	2 %	16.5 M	16.5 M	16.7 M	33.0 M
	5 %	12.4 M	12.4 M	12.6 M	24.9 M
	10 %	9.7 M	9.7 M	9.8 M	15.7 M
T_{mem}	0 %	2.55 Mb	0.24 Mb	1.77 kb	2.5 kb
	1 %	855 kb	2.3 kb	1.77 kb	2.5 kb
	2 %	700 kb	2.3 kb	1.77 kb	2.5 kb
	5 %	529 kb	2.3 kb	1.77 kb	2.5 kb
	10 %	415 kb	2.3 kb	1.77 kb	2.5 kb
			"scalar"		
T_{op}	0 %	60.1 M	60.2 M	2586 M	130 M
	1 %	20.1 M	20.1 M	22.1 M	41.1 M
	2 %	16.5 M	16.5 M	17.7 M	33.5 M
	5 %	12.4 M	12.4 M	13.2 M	25.3 M
	10 %	9.7 M	9.7 M	10.3 M	19.8 M
T_{mem}	0 %	2.55 Mb	2.34 Mb	1.77 kb	2.5 kb
	1 %	855 kb	500 kb	1.77 kb	2.5 kb
	2 %	700 kb	395 kb	1.77 kb	2.5 kb
	5 %	529 kb	299 kb	1.77 kb	2.5 kb
	10 %	415 kb	241 kb	1.77 kb	2.5 kb

The required memory as well as the number of operations in the basic algorithm scales linearly with the number of hysterons, hence the reduction of hysterons is of course beneficial from both points of view. All algorithms take benefit from the simplification of the set of hysterons, but the improvement is particularly remarkable for the memoryless algorithm, for which a decrease of the computational time of nearly two orders of magnitude is observed. This is due to the fact that the simplification procedure seems to remove mostly hysterons which are frozen for the most of time. Thus the fraction f of frozen hysterons is strongly decrease (Figure 9), and hence the time complexity of the memoryless and pooled algorithms is decreased as well (Table 1).

The benefit is less pronounced for the incremental algorithm, but still it is clearly visible. Surprisingly, for $p = 0.05$ and $p = 0.1$ the incremental algorithm generally has a computational cost higher than the memoryless algorithm. This can be explained by the fact that the incremental algorithm needs to evaluate the unit magnetization at the current time step, but also at the previous time step[3]. Hence, when the fraction of frozen hysteron f is low enough so that it becomes comparable to f_u, the memoryless algorithm becomes even more competitive than the incremental one. From the standpoint of the occupied memory, the memoryless and incremental algorithms take no benefit from the simplification of the set of hysterons; nevertheless, these algorithms still outperform both the basic and the pooled algorithms.

Notice that this effect depends strongly on the type of signals, and it is unsurprisingly more pronounced in the case of the signal "harmonics", which comes quickly to a steady state where most of the hysterons are unfrozen. Conversely, in the case of the signal "scalar" where the applied magnetic field vanishes several times, this effect is somehow reduced, but still it is clearly visible.

From the standpoint of FEA, this effect could make the pooled and memoryless algorithms competitive with respect of the basic algorithm. However, it has to be noticed that the virgin state is problematic because of the high fraction of frozen hysterons.

[3] This is necessary to determine whether hysterons undergo a transition frozen/unfrozen. Unfortunately the unit polarization at the previous step cannot be stored in memory, otherwise all benefits of the algorithm from the standpoint of memory occupation would be wasted.

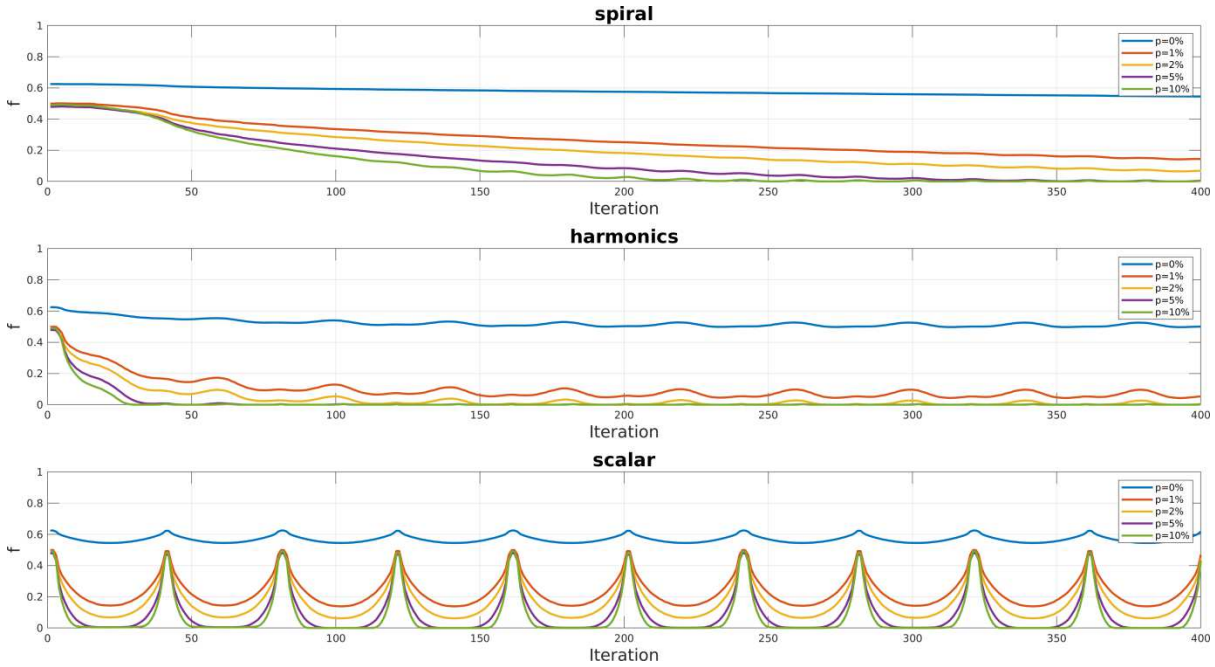

Figure 9. Evolution of the fraction *f* of frozen hysterons during the simulations (material #1) obtained for several values of *p*. Even small values of *p* reduce significantly the fraction *f* of frozen hysterons.

Incremental algorithm with reduced models

Reduced models have been devised to be employed mainly with the incremental algorithm. At each step of the algorithm, and for each computational point, a reduced model is searched in a pool which is enriched dynamically – that is, if no suitable reduced model is found in the pool, a new model is created on-the-fly and added to the pool.

The parameters which control the creation of new reduced models are the size ρ of the validity domain, the threshold distance h_{min} and the number of clusters N_C. The size ρ of the domain of validity $\mathrm{B}(\mathbf{Ha}_0, \rho)$ of reduced models depends on the applied magnetic field in the current $\mathbf{Ha}_n$ and the second-to-last one $\mathbf{Ha}_{n-1}$, and on the magnitude of the applied field:

$$\rho = \max\{\rho_{min}, \frac{2\pi\|\mathbf{Ha}\|}{N_\rho}, \|\mathbf{Ha}_n - \mathbf{Ha}_{n-1}\|\} \tag{22}$$

A minimal size $\rho_{min} = 20\,\mathrm{A/m}$ is imposed in order to avoid the unnecessary creation of reduced models with tiny validity domain. The parameters N_ρ represents the minimal number of reduced models used to cover closed cycle of the applied magnetic field. The validity domain of new reduced models is centred in $\mathbf{Ha}_n$, so Equation 22 guarantees that $\mathbf{Ha}_n$ and $\mathbf{Ha}_{n-1}$ belong to the validity domain. The threshold distance has been chosen proportionally to $\mathbf{Ha}_n$:

$$h_{min} = \chi\|\mathbf{Ha}\| \tag{23}$$

For each set of parameters (N_ρ, χ, N_C), we compute the errors e_{max} and e_{rel} defined in Equations 20 and 21 respectively. Also, it is interesting to track the total number of reduced

models and the occupied memory for the pool of reduced models. Some statistics are presented in Table 6 (material #1) and Table 7 (material #2) for the reference set of parameters: $N_\rho = 40$, $\chi = 1.2$, $N_C = 32$. Simulations have been run by using a simplified set of hysterons with $p = 2\%$. The total number of elementary operations T_{OP}, and the "net" number which does not include the creation of reduced models (RM) are provided. Notice that in principle reduced models could be generated off-line once for all.

Table 6: Statistics of the simulation by using the incremental algorithm with reduced models (material #1). Simulation parameters are: $N_\rho = 40$, $\chi = 1.2$, $N_c = 32$ and $p = 2$ % (M = 10^6 elementary operations).

	"spiral"	"harmonics"	"scalar"
e_{max}	2.55 %	1.00 %	0.77 %
e_{rel}	2.60 %	1.04 %	0.57 %
T_{op}	4.50 M	2.36 M	3.84 M
T_{op} (generation of RM excluded)	2.98 M	1.30 M	2.69 M
T_{op} incremental algorithm without RM	15.60 M	14.74 M	15.29 M
T_{op} basic algorithm	7.23 M	7.23 M	7.23 M
Nb reduced models	113	71	101
Average Nb of hysterons	2083	1392	2633
Occupied memory	262 kb	286 kb	181 kb

Table 7: Statistics of the simulation by using the incremental algorithm with reduced models (material #2). Simulation parameters are: $N_\rho = 40$, $\chi = 1.2$, $N_c = 32$ and $p = 2$ % (M = 10^6 elementary operations).

	"spiral"	"harmonics"	"scalar"
e_{max}	1.9 %	1.0 %	1.5 %
e_{rel}	9.5 %	8.5 %	3.9 %
T_{op}	8.56 M	3.4 M	7.0 M
T_{op} (generation of RM excluded)	4.26 M	0.78 M	3.65 M
T_{op} incremental algorithm without RM	33.70 M	33.0 M	33.5 M
T_{op} basic algorithm	16.46 M	16.46 M	16.46 M
Nb reduced models	113	71	101
Average Nb of hysterons	2545	967	6026
Occupied memory	656 kb	661 kb	356 kb

In Figure 10 is depicted the magnetization $\mathbf{M}$ for the "spiral" signal, computed with material #1 by using the basic algorithm (reference) and the incremental algorithm with reduced models. One observes that the error is quite acceptable, and it is mainly located close to the virgin state (see the zoom in the inset). For this signal, 113 reduced models have been created. Reduced models are composed of 2083 hysterons in average for the material #1 (to be compared with the 18033 hysterons of the simplified set, and with the 134000 of the original set). The number of hysterons depends on the domain of validity of reduced models: the highest number (N = 4158) is found close to the virgin state, whereas for $\|\mathbf{Ha}\| > 100$ A/m the number of hysterons for each reduced model is steadily under the average. A similar trend is observed for the material #2. However, it is worth observing that

the couple material/signal strongly determines the extent of the economy obtained by using reduced models.

Depending on the signal and on the material, the memory required to store the pool of reduced models is of about 500 kb (order of magnitude). The occupied memory may appear rather high, but we stress that the pool of reduced models is common to all computational points. In order to appreciate the practical consequences of memory occupation of the pool of reduced models, algorithms should be plugged into a FEA software, where a high number of points have to be computed at each time step, with a substantial scaling economy.

The number of elementary operations is reduced with respect of the incremental algorithm when reduced models are not used, and it is usually much lower with respect of the basic algorithm. The gain is even bigger if one takes out the computations required to create reduced models, which can eventually done off-line. However, one should keep in mind that the number of elementary operations is not fully representative of execution time, in that the algorithms which have to be implemented for the incremental algorithm and to handle the pool of reduced models are much more complex with respect of the basic algorithm. Nevertheless, data reported in Tables 6 and 7 suggest that the incremental algorithm with reduced models may indeed be competitive with the basic algorithm in terms of both space and even time complexity.

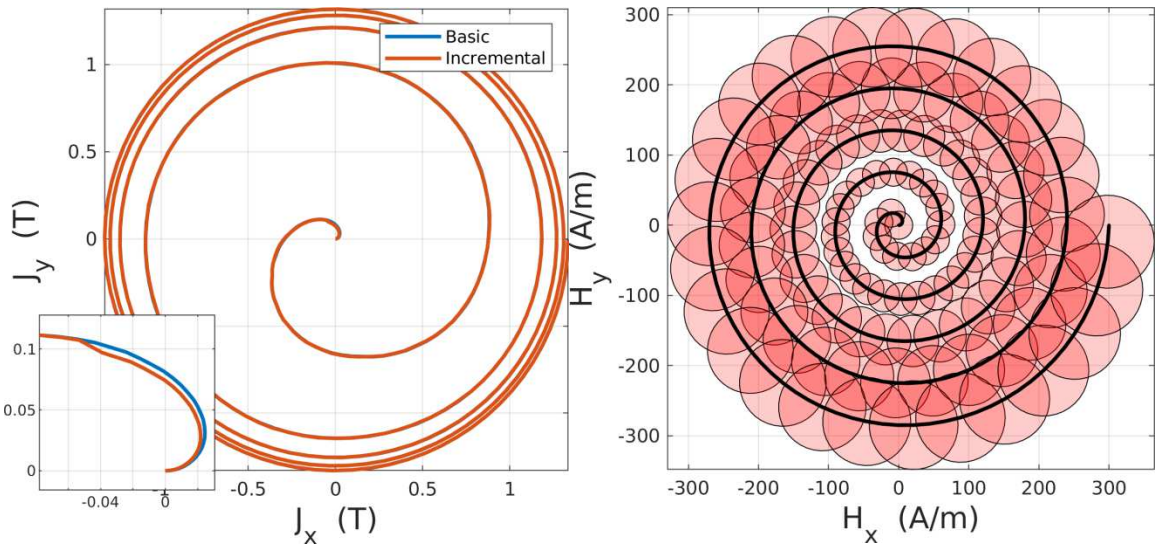

Figure 10. Left: magnetization computed by using the basic algorithm and the incremental algorithm which makes use of reduced models ($N_\rho = 40$, χ=40, N_C=32). The inset shows a zoom of the **J**-plane close to the virgin state, where a moderate discrepancy between the two algorithms can be observed. Right: validity domain of the reduced models.

The effect of clustering at several time steps are depicted in Figure 11. Clusters are depicted by using patches of different colours. One observes that clusters correspond to different "sectors" of the plane, which converge toward the computational point (in order to have a readable image, the number of clusters have been purposely reduced to generate this figure). An "exclusion zone" where no hysteron is clustered can be observed in the neighbourhood of the computational point. The extent of the exclusion zone is determined by the parameter χ, and it is motivated by the necessity of reducing the error on unit polarization (Equation 18).

Qualitatively similar results are obtained by using the two other signals. A very small variability in the statistics is observed by repeating the simulations with the same parameters. This variability, which is barely observable, is explained by the random initialization of the k-means algorithm, and doesn't alter the overall conclusions. Conversely, the number of

reduced models is solely determined by the signal and the set of parameters used to drive simulations, namely ρ_{min} and N_ρ.

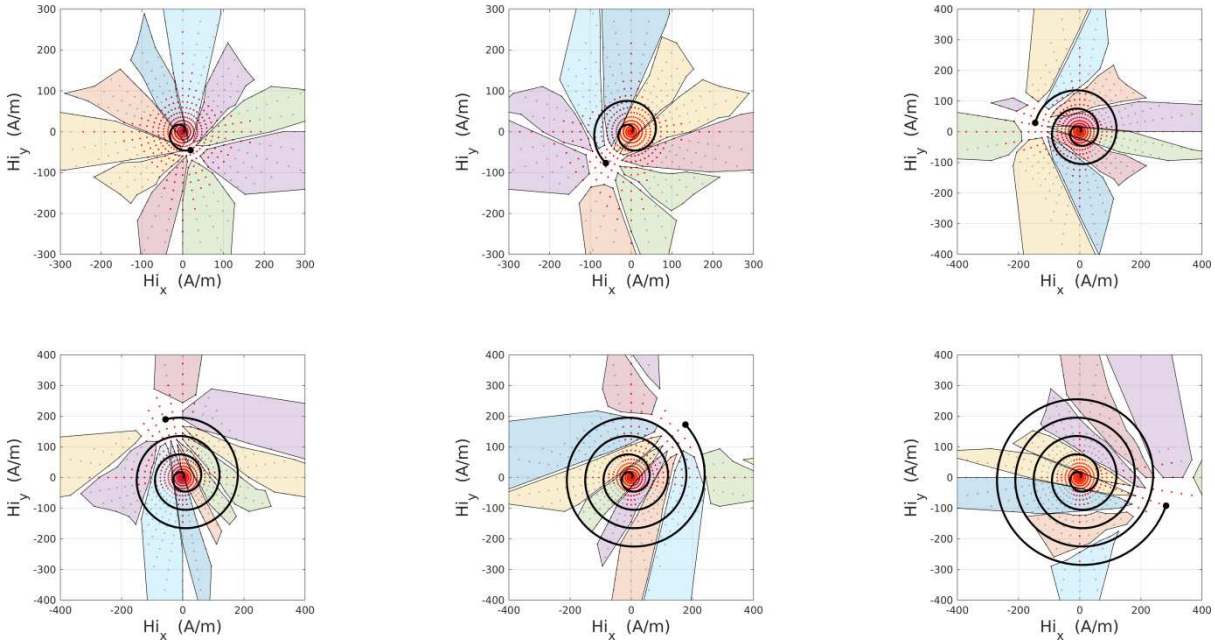

Figure 11. Clusters of hysterons at several time steps (N_C = 10) for the signal "spiral" (material #1). Red spots represent hysterons which have been conserved in the reduced model; grey spots represent the original hysterons (a single spot may correspond to several hysterons with different radius).

The effect of parameters χ and N_c on the results are presented hereafter. When χ, and thus h_{min}, is increased, the error on the unit polarization decreases (Equation 18). Hence the computed error decreases, while the number of average hysterons of reduced models and the number of elementary operations both increase (Table 8).

Table 8: Effect of variations of the parameter χ. Simulation parameters are: N_ρ = 40, N_c = 32 and p = 2 %. The number of operations T_{op} include the generation of reduced models (M = 10^6 elementary operations).

	χ	"spiral"		"harmonics"		"scalar"	
Material		#1	#2	#1	#2	#1	#2
e_{max}	1	3.0 %	2.2 %	1.6 %	1.0 %	1.7 %	1.5 %
	1.2	2.7 %	1.9 %	1.6 %	1.0 %	1.7 %	1.6 %
	1.5	2.4 %	1.7 %	1.6 %	0.98 %	1.6 %	1.5 %
	2	2.2 %	1.3 %	1.5 %	0.99 %	1.6 %	1.6 %
	3	1.8 %	1.0 %	1.5 %	1.00 %	1.6 %	1.5 %
e_{rel}	1	53 %	11 %	9.3 %	10 %	10 %	4.4 %
	1.2	11 %	9.1 %	9.2 %	8.6 %	8.6 %	3.7 %
	1.5	10 %	11 %	6.7 %	6.7 %	6.1 %	3.3 %
	2	16 %	4.8 %	3.8 %	4.2 %	4.1 %	2.7 %
	3	4.3 %	2.3 %	2.6 %	2.17 %	2.8 %	2.6 %
T_{op}	1	4.33 M	8.19 M	2.22 M	3.30 M	3.66 M	6.72 M
	1.2	4.50 M	8.56 M	2.36 M	3.40 M	3.84 M	7.03 M
	1.5	4.79 M	9.17 M	2.58 M	3.51 M	4.12 M	7.47 M
	2	5.31 M	10.3 M	3.07 M	3.8 M	4.64 M	8.34 M
	3	6.56 M	13.3 M	4.65 M	4211	5.97 M	10.89 M
Average	1	1829	2131	1132	830	2347	5285
number of	1.2	2083	2545	1392	967	2633	6026

hysterons	1.5	2495	3252	1657	1226	3082	7175
	2	3207	4683	2335	1777	3853	9118
	3	5247	9178	4438	4211	5651	14314

Unsurprisingly, it is observed that the error is lowered by increasing the number of clusters N_C (Table 9). The number of operations is not substantially modified, because the increase in the number of hysterons which have to be handled is quite negligible with respect of the average number of hysterons of reduced models. For high values of N_C we seldom experience problems with the convergence of the k-means algorithm. These problems, which could be solved by tweaking the parameters of the clustering algorithm (k-means), don't seem to affect the accuray of the results.

Table 9: Effect of the number of hysterons on the accuracy Simulation parameters are: $N_\rho = 40$, $\chi = 1.2$ and $p = 2$ %. [*] indicates problems with the convergence of the k-means algorithm.

	N_C	"spiral"		"harmonics"		"scalar"	
Material		#1	#2	#1	#2	#1	#2
e_{max}	8	5.59 %	2.36 %	2.11 %	1.38 %	3.15 %	1.78 %
	16	3.45 %	2.1 %	1.71 %	1.08 %	1.64 %	1.57 %
	32	2.68 %	2.0 %	1.63 %	1.04 %	1.68 %	1.54 %
	[*] 64	2.24 %	1.9 %	1.63 %	0.98 %	1.64 %	1.53 %
e_{rel}	8	143 %	154 %	9.4 %	17 %	19 %	4.0 %
	16	84 %	8.6 %	15 %	9.1 %	10 %	3.9 %
	32	10 %	16 %	7.3 %	8.9 %	8.5 %	3.9 %
	[*] 64	10 %	9.3 %	8.7 %	8.7 %	8.5 %	3.7 %

Memoryless algorithm with reduced models

The generation of reduced models, which was devised to accelerate the incremental algorithm, can be modified in order to be used with other algorithms. To this aim, it is enough to leave all frozen hysterons in the reduced models, including those who are and remain frozen $\forall \mathbf{Ha} \in \mathrm{B}(\mathbf{Ha}_0, \rho)$ (case iii, Figure 6). The result of simulations taken on by using the memoryless algorithm are reported in tables 10 (material #1) and 11 (material #2).

Table 10: Statistics of the simulation by using the memoryless algorithm with reduced models (material #1). Simulation parameters are: $N_\rho = 40$, $\chi = 1.2$, $N_c = 32$ and $p = 2$ % (M = 10^6 elementary operations).

	"spiral"	"harmonics"	"scalar"
e_{max}	2.21 %	1.55 %	1.61 %
e_{rel}	6.95 %	2.00 %	2.37 %
T_{op}	181 M	9.3 M	85 M
T_{op} (generation of RM excluded)	179 M	7.0 M	83 M
T_{op} memoryless algorithm without RM	184 M	14 M	89 M
T_{op} basic algorithm	7.23 M	7.23 M	7.23 M
Nb reduced models	151	133	109
Average Nb of hysterons	3919	1360	4888
Occupied memory	267 kb	294 kb	268 kb

Table 11: Statistics of the simulation by using the memoryless algorithm with reduced models (material #2). Simulation parameters are: $N_\rho = 40$, $\chi = 1.2$, $N_c = 32$ and $p = 2$ % (M = 10^6 elementary operations).

	"spiral"	"harmonics"	"scalar"
e_{max}	1.71 %	1.00 %	1.53 %
e_{rel}	6.52 %	1.40 %	3.17 %
T_{op}	41.2 M	5.9 M	6.6 M
T_{op} (generation of RM excluded)	18.0 M	0.58 M	2.6 M
T_{op} memoryless algorithm without RM	32.4 M	16.7 M	17.7 M
T_{op} basic algorithm	16.5 M	16.5 M	16.5 M
Nb reduced models	151	133	109
Average Nb of hysterons	2229	666	4239
Occupied memory	662 kb	663 kb	660 kb

The obtained results are deceiving: in general, the usage of reduced models is quite ineffective in reducing the number of elementary operations, with the only exception of the signal "harmonics" simulated with material #2. This can be explained by the necessity of handling all frozen hysterons when using the memoryless algorithm.
The case of the pooled algorithm has not been explored in this work. However, one can foresee an additional complexity which consists in handling the transition from a reduced domain to another, which is far from being a simple task. Most importantly, the main issue with this algorithm is the memory occupation, which is not solved by using reduced models.

On the saturation and congruency properties

The four algorithms presented in this work compute exactly the same result (up to rounding errors due to floating point arithmetic); hence they don't alter at all the properties of congruency and the behaviour of the material in the case of saturation (see [15] for a detailed explanation of these properties).
Conversely, simplification of the set of hysterons and reduced models introduce approximations. Simplification of the set of hysterons ends up in creating a "lightweight" model which has the same behaviour of the original model, up to an acceptable approximation (Equation 10). Hence it preserves the congruency property, which is intrinsic to the Preisach model. The value of the polarization at saturation can be modified to a little extent, unless the weights are renormalized (Equation 11).
As for reduced models, it has to be observed that the approximation concerns only the contribution of unfrozen hysterons; hence the congruency property and the behaviour of the material at saturation are not modified. By the way, the approximation introduced by using reduced models is more effective precisely when the material is saturated, because clustered hysterons are "far" from the applied field **Ha**, thus the angle $\gamma$is very small (Equation 18).
These observations are confirmed by numerical simulations. For both materials, we simulated the saturation, followed by three minor loops. The obtained results obtained with all algorithms are plotted in Figure 12, together with the reference case (computed by using the basic algorithm with the original set of hysterons, without using reduced models). There is of course an approximation, but one observes that there is no effect on the congruency property, nor on the saturation.

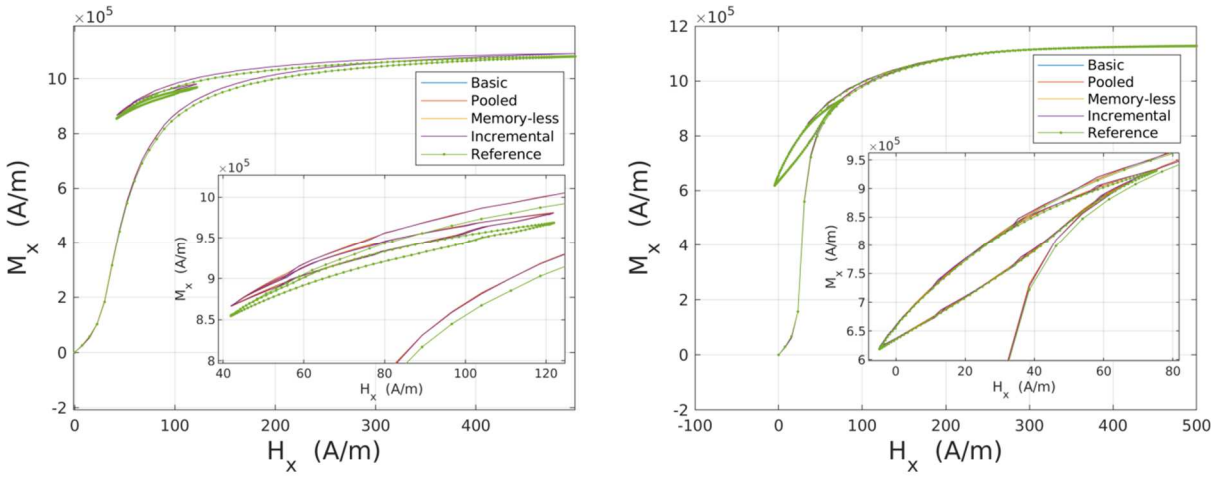

Figure 12. Signal with minor loops for the material #1 (left) and for the material #2 (right). Each loop is repeated three times. One observes that all four algorithms provide the same result, which is close to the reference one, and verify the congruency property (inset: all loops are perfectly superposed). Algorithms run on simplified materials (p = 2 %) with renormalization of weights; the incremental algorithm makes use of reduced models (χ = 1.2, N_c = 32, N_p = 40).

Conclusions

In this work four algorithms, which all implement the Vector Hysteresis Model, are presented and critically compared. Apart from the basic algorithm, which is classical, the three other algorithms (named pooled, memoryless and incremental) all aim at reducing the memory occupation in view of simulating a real model with Finite Element analysis (FEA). The pooled algorithm is a variant of the basic algorithm, which allows a considerable economy of memory at the price of a more complex implementation. Conversely, the memoryless and incremental algorithms reduce of several orders of magnitude the memory occupation, at the price of a much higher computational cost. In order to reduce to an acceptable level the computational cost of these two algorithms, the generation and usage of reduced models is devised. Moreover, a simplification procedure which allows to dramatically reduce the number of hysterons of a given model has been implemented.

The time and space complexity of all algorithms are predicted theoretically and validated through numerical experiments on two artificial magnetic materials and three different vector excitations (signals). The obtained data clearly demonstrate that the pooled algorithm requires a very high amount of memory when materials are excited with a low magnetic field, because in this case, a very high fraction of hysterons are frozen. This kind of situation is typically found in the first time steps of FE simulations, where the material is in the virgin state. Conversely, the first time steps are very cheap in the case of memoryless and incremental algorithms. Hence, one could devise a computational strategy which consists in starting the simulation by using the memoryless or the incremental algorithm, then switch to the pooled algorithm when the fraction of frozen hysterons is low enough.

The usage of the simplification procedure, which could indeed be considered as a step of the identification procedure, is mandatory in that it is extremely effective in reducing both the computational cost and memory consumption. With the materials used in our numerical experiments, a very large part of the original hysterons are removed at the price of a very low error (of the order of a few percent), which is usually compatible with the practical experimental error, and with the intrinsic uncertainties in the material characterization.

Finally, the usage of simplified models together with the incremental algorithm achieve a reduction of several orders of magnitudes of the memory occupation, and also a reduction of the number of elementary operations required to simulate the material. We must warn that the presented results on the time complexity are strongly influenced by the present implementation of the algorithms, which is not at all optimized for speed, especially in as much as the incremental algorithm is concerned. However, if the theoretical results should be confirmed in practice, the incremental algorithm with reduced models could be a game-changer in the usage of the Vector Hysteresis Model in FEA simulation of large electrical systems.

While waiting for an optimized implementation of the algorithms, other paths can be devised to reduce the computational cost of the memoryless and incremental algorithms. The main point is that with these algorithms the state of the material is represented by its full history, that is by all the past values of the applied magnetic field. If one could devise a strategy to truncate the history which has to be taken into account, this would reduce proportionally the computational time, which is these algorithms is dominated by the search back in time of the time step when hysterons got frozen. Another point which deserves investigation is how to handle the case of periodic signals. This is particularly relevant to simulate the steady state of electrical systems by using standard harmonic formulations or the harmonic balance technique.

Conflicts of Interest

The authors declares that there is no conflict of interest regarding the publication of this paper.

References

[1] Jiles, D. C.; Atherton, D. L., "Ferromagnetic Hysteresis", IEEE Trans. Magn. 1983, 19 (5), 2183-2185, https://doi.org/10.1016/0304-8853(86)90066-1.

[2] Jiles, D. C.; Atherton, D. L., "Theory of Ferromagnetic Hysteresis", J. Appl. Phys. 1984, 55, 2115, https://doi.org/10.1063/1.333582

[3] Jiles, D. C.; Atherton, D. L., "Theory of Ferromagnetic Hysteresis", J. Magn. Magn. Mater. 1986, 61, 48-60, http://dx.doi.org/10.1016/0304-8853(86)90066-1

[4] Jiles, D. C.; Atherton, D. L., "A Model of Ferromagnetic Hysteresis", J. Magn. Magn. Mater., 1986, 61.

[5] Bobbio, S.; Marrucci, G., "A Possible Alternative to Preisach's Model of Static Hysteresis", II Nuovo Cimento 1993, 15-D (5), 723-734,

[6] Visintin, A., "Differential Models of Hysteresis", Springer Verlag: New York, 1994, https://doi.org/10.1007/978-3-662-11557-2

[7] Bobbio, S.; Miano, G.; Serpico, C.; Visone, C. "Models of Magnetic Hysteresis Based on Play and Stop Hysterons", IEEE Trans. Magn. Nov. 1997, 33 (11), 4417-4426, DOI 10.1109/20.649875

[8] Bergqvist, A.; Lundgren, A.; Engdahl, G., "Experimental Testing of an Anisotropic Vector Hysteresis Model", IEEE Trans. Magn. Sep. 1997, 33 (5), 4152-4154, DOI 10.1109/20.619693

[9] Cardelli, E.; Della Torre, E., "Modelling of Hysteresis and Dynamic Losses in Soft Ferrites up to Radiofrequency Level", Physica B 2001, 306 (1e4), 240-245, DOI 10.1016/S0921-4526(01)01011-0

[10] F. Preisach, "Uber die magnetische Nachwirkung", Zeitschrift fur Physik, vol. 94, pp. 277-302, 1935, https://doi.org/10.1007/BF01349418

[11] Mayergoyz, I. D. *Mathematical Models of Hysteresis,* Springer-Verlag: New York, 1991, https://doi.org/10.1007/978-1-4612-3028-1

[12] Della Torre, E. *Magnetic Hysteresis*, IEEE Press: New York, 1999, https://ieeexplore.ieee.org/servlet/opac?bknumber=5265195

[13] Della Torre, E., Pinzaglia, E., Cardelli, E., "Vector modeling - Part I: Generalized hysteresis model", Physica B: Condensed Matter, vol. 372, no. 1-2, pp. 111-114, 2006, https://doi.org/10.1016/j.physb.2005.10.028

[14] Della Torre, E., Pinzaglia, E., Cardelli, E., "Vector modeling - Part II: Ellipsoidal vector hysteresis model. Numerical application to a 2D case", Physica B: Condensed Matter, vol. 372, no. 1-2, pp. 115-119, 2006, DOI:10.1016/j.physb.2005.10.029
[15] Cardelli, E., "A general hysteresis operator for the modeling of vector fields", IEEE Transactions on Magnetics, vol. 47, no. 8, pp. 2056-2067, 2011, DOI:10.1109/TMAG.2011.2126589
[16] Cardelli, E., Torre, E.D., Faba, A., "A general vector hysteresis operator: Extension to the 3-D case", IEEE Transactions on Magnetics, vol. 46, no. 12, pp. 2056-2067, 2010, DOI:10.1109/TMAG.2010.2072933
[17] Cardelli, E., "Advances in Magnetic Hysteresis Modeling", Handbook of Magnetic Materials, vol. 24, pp. 323-409, 2015, https://doi.org/10.1016/bs.hmm.2015.10.002
[18] Cardelli, E., Carpentieri, M., Della Torre, E., Drisaldi, G., Faba, A., "Magnetization dependent vector model and single domain nanostructures", Journal of Applied Physics, vol. 105, no. 7, art. no. 07D516, 2009, https://doi.org/10.1063/1.3068009
[19] Cardelli, E., Della Torre, E., Faba, A., "Properties of a class of vector hysteron models", Journal of Applied Physics, vol. 103, no. 7, art. no. 07D927, 2008, https://doi.org/10.1063/1.2833758
[20] Cardelli, E., Della Torre, E., Faba, A., "Numerical implementation of the DPC model", IEEE Transactions on Magnetics, vol. 45, no. 3, pp. 1186-1189, 2009, DOI: 10.1109/TMAG.2009.2012549
[21] MacQueen, James. "Some methods for classification and analysis of multivariate observations. " Proceedings of the fifth Berkeley symposium on mathematical statistics and probability. Vol. 1. No. 14. 1967, https://www.bibsonomy.org/bibtex/25dcdb8cd9fba78e0e791af619d61d66d/enitsirhc
[22] Maxime Tousignant. « Modelisation de l'hysteresis et des courants de Foucault dans les circuits magnetiques par la methode des elements finis ». Energie électrique. Université Grenoble Alpes; Ecole Polytechnique (Montréal, Canada), 2019. Français. NNT: 2019GREAT065. tel-02905410
[23] Tousignant, M., Sirois, F., Meunier, G., & Guerin, C. (2019). "Incorporation of a Vector Preisach–Mayergoyz Hysteresis Model in 3-D Finite Element Analysis". IEEE Transactions on Magnetics, 55(6), 1-4, DOI: 10.1109/TMAG.2019.2900690
[24] Zhu, L., Wu, W., Xu, X., Guo, Y., Li, W., Lu, K., & Koh, C. S. (2019). An improved anisotropic vector Preisach hysteresis model taking account of rotating magnetic fields. IEEE Transactions on Magnetics, 55(6), 1-4, DOI: 10.1109/TMAG.2019.2899592
[25] Adly, A. A., and I. D. Mayergoyz. "A new vector Preisach-type model of hysteresis." Journal of applied physics 73.10 (1993): 5824-5826, https://doi.org/10.1063/1.353539
[26] Dlala, E., Belahcen, A., Fonteyn, K. A., & Belkasim, M. (2009). Improving loss properties of the Mayergoyz vector hysteresis model. IEEE Transactions on Magnetics, 46(3), 918-924, DOI: 10.1109/TMAG.2009.2034846
[27] Hussain, Sajid, and David A. Lowther. "An efficient implementation of the classical Preisach model." IEEE Transactions on Magnetics 54.3 (2017): 1-4, DOI: 10.1109/TMAG.2017.2748100
[28] Dupre, L., & Melkebeek, J. (2003). Electromagnetic hysteresis modelling: from material science to finite element analysis of devices. International Compumag Society Newsletter, 10(3), 4-15.
[29] Guérin, C., Jacques, K., Sabariego, R.V., Dular, P., Geuzaine, C., Gyselinck, J., 2017. Using a Jiles-Atherton vector hysteresis model for isotropic magnetic materials with the finite element method, Newton-Raphson method, and relaxation procedure: Using a vector Jiles-Atherton hysteresis model. International Journal of Numerical Modelling: Electronic Networks, Devices and Fields 30, e2189. https://doi.org/10.1002/jnm.2189.
[30] Jacques, K. Energy-based magnetic hysteresis models-theoretical development and finite element formulations. 2018. PhD Thesis. Université de Liège, Liège, Belgique.
[31] Leite, J. V., Benabou, A., Sadowski, N., Clenet, S., Bastos, J. P. A., & Piriou, F. (2008). Implementation of an anisotropic vector hysteresis model in a 3-D finite-element code. IEEE transactions on magnetics, 44(6), 918-921, DOI: 10.1109/TMAG.2007.915810
[32] S. Quondam Antonio, A.M. Ghanim, A. Faba, A. Laudani, Numerical simulations of vector hysteresis processes via the Preisach model and the Energy Based Model: An application to Fe-Si laminated alloys, Journal of Magnetism and Magnetic Materials, Volume 539, 2021,168372, ISSN 0304-8853, https://doi.org/10.1016/j.jmmm.2021.168372